MODELLING FRAMEWORK FOR FLIGHT DYNAMICS OF FLEXIBLE AIRCRAFT

Vilius PORTAPAS[1], Alastair COOKE[2], Mudassir LONE[3]

[1,2,3]Centre for Aeronautics, School of Aerospace, Transport and Manufacturing, Cranfield University, College Road, MK43 0AL, Cranfield, UK
E-mails: [1]v.portapas@cranfield.ac.uk (corresponding author); [2]a.cooke@cranfield.ac.uk; [3]m.m.lone@cranfield.ac.uk

Received and accepted dates

Abstract. Flight dynamics and handling qualities of any flexible aircraft can be analysed within Cranfield Aircraft Accelerated Loads Model (CA^{2}LM) framework. Modelling techniques and methods used to develop the framework are presented. Aerodynamic surfaces were modelled using Modified Strip Theory (MST) and a state-space representation to model unsteady aerodynamics. With a modal approach the structure flexibility and each mode's influence on structure deflections are analysed. To supplement the general overview of the framework equations of motion, atmosphere, gravity, fuselage and engines models are introduced. The AX-1 general transport aircraft model is analysed as an example of the CA^{2}LM framework capabilities. Results showed that according to Gibson Dropback criterion the aircraft with no control system lacks of stability and its longitudinal handling qualities are unsatisfactory. Finally, steps for future developments of CA^{2}LM framework are listed within conclusions.

Keywords: aeroelastics, flexible aircraft, flight dynamics, handling qualities.

Introduction

Airframe flexibility effects have always been of concern to aircraft designers. As a consequence manufacturers have developed extensive loads and aeroelastic analysis processes aimed to minimise airframe weight, develop technologies to achieve environmental targets (European Commission 2011, Tollefson 2016) and satisfy safety requirements set by the regulatory authorities. However, for the design of traditional aircraft, these processes are usually decoupled from the flight dynamic analysis and assessments. This has been justified by the relatively small size and high stiffness of the traditional airframe. With the advent of modern large transport and high altitude long endurance (HALE) aircraft, where extensive use of advanced materials has led to large and light weight flexible airframes, the interaction between flight dynamics and aeroelasticity has become a more significant design driver. Flight dynamic analysis methods can no longer assume a rigid airframe and aeroelasticity practices cannot ignore rigid body flight dynamics.

Modelling frameworks of various complexity have been developed both in industry and academia. Industrial frameworks are highly complex and aimed at supporting certification activities. These often couple computational fluid dynamics (CFD) with computational structural mechanics (CSM) and result in processes that provide the desired insight, but are computationally very expensive (Cooper et al. 2016, Lindhorst et al. 2014, Wang et al. 2015). Reduced order models such as VARLOADS (Kier et al. 2005) have also been developed, but these have only seen limited research usage. In academia, Palacios et al. (Palacios et al. 2010, Palacios and Cesnik 2008, Simpson et al. 2015) have shown the capability to link aeroelasticity with flight control and develop novel approaches to aeroservoelastic analysis of highly flexible configurations. Structural flexibility effects were modelled through the implementation of a nonlinear structural dynamics formulation. Aerodynamic contributions were captured through the implementation of an unsteady vortex lattice method code. Although the approach adopted by Palacios et al is computationally cheaper than those used in industry, real time simulation is still not possible.

The Cranfield Aircraft Accelerated Loads Model (CA^{2}LM) framework was initially developed for the evaluation of handling qualities of large flexible aircraft (Andrews, 2011; Lone, 2013). It also provides the capability for flight control law design and reduced order aeroservoelastic analysis of user defined airframe configurations. This article provides a brief overview of this modelling framework and its components, along with examples demonstrating its use for flight loads and handling qualities analysis.

1. Overview of the CA^{2}LM framework

The CA^{2}LM framework provides an environment for the modelling and simulation of flexible aircraft (of various configurations) in MATLAB/Simulink. This not only allows the framework to be easily linked with in-house flight control toolboxes and open source codes such as SIDPAC (Morelli 2002) for system identification, it also allows the potential for connections with the flight simulation facilities available at Cranfield University. The framework was initially developed for modelling the AX-1 configuration (shown in Fig. 1). Since then, the framework has seen

numerous upgrades and is now known as the CA^{2}LM framework. This section discusses the high level structure of the framework and techniques implemented to model aerodynamics, structural dynamics and the equations of motion. The AX-1 configuration will be used to demonstrate the capabilities of this simulation framework.

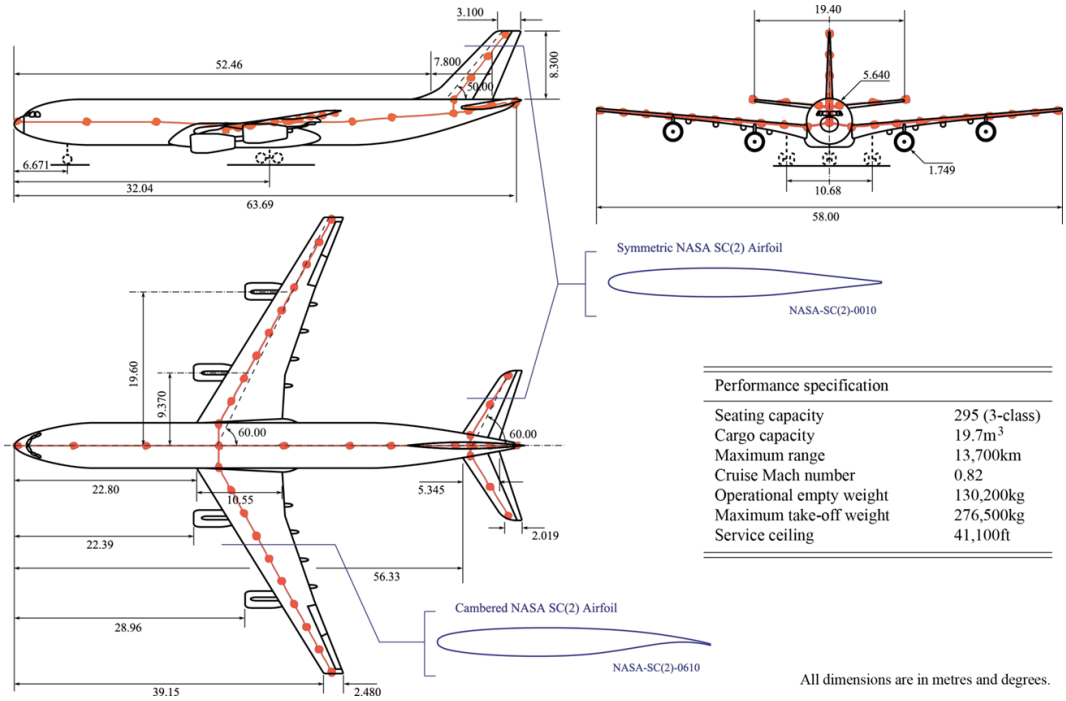

Performance specification	
Seating capacity	295 (3-class)
Cargo capacity	19.7m^3
Maximum range	13,700km
Cruise Mach number	0.82
Operational empty weight	130,200kg
Maximum take-off weight	276,500kg
Service ceiling	41,100ft

Fig. 1. AX-1 aeroplane model and its specifications.

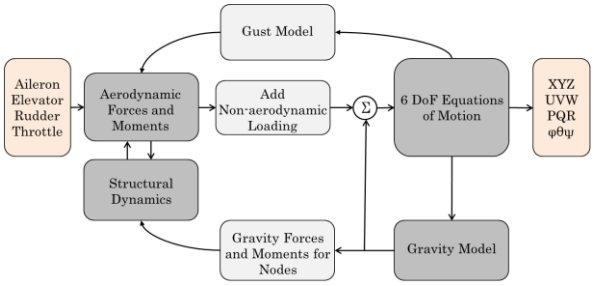

Fig. 2. Structure of CA^{2}LM framework.

The overall structure of CA^{2}LM framework is shown in Fig. 2. The user can provide time domain signals representing inputs such as aileron, elevator, rudder and throttle variations. The outputs are aircraft rigid body states such as aircraft position in the Earth axis, its angular and translational velocities and attitude in the body axis. Internal structural loads such as bending moments and torsion can also be output. The core of the framework consists of the aerodynamic, structural, gravity and equations of motion blocks. These are discussed separately below. The gust/turbulence block provides an environment for modelling atmospheric disturbances and allows the implementation of continuous turbulence and discrete gusts. The non-aerodynamic loading block allows the specification of specific mass properties. Fuel, cargo and passenger loadings can be specified in detail and this information is used to calculate aircraft mass, inertia tensor and centre of gravity position.

1.1. Modelling of aerodynamic surfaces

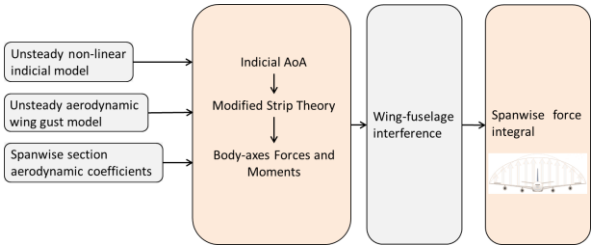

Fig. 3. Aerodynamic modelling of aerodynamic surfaces in CA^{2}LM framework.

The aerodynamic modelling process is further detailed in Fig. 3. The wings, tailplanes and the fin are modelled in very similar ways. However, a block, modelling interference effects between the lifting surfaces and the fuselage is added to the wing aerodynamics. Steady aerodynamic forces and moments are modelled using a Modified Strip Theory approach that relies on the input of appropriate aerofoil aerodynamic characteristics as a function of airspeed and angle of attack. This enables the calculation of aerodynamic forces on a user defined wing planform and takes into account compressibility effects via the Prandtl-Glauert correction factor (DeYoung and Harper 1948; Weissinger 1947). A Leishman-Beddoes unsteady aerodynamic model has been implemented in steady-state form. Therefore, the entire airframe is divided into strips and each strip has a focal point about which forces and moments are calculated. These are referred to as the aerodynamic nodes.

The implementation of unsteady aerodynamics model is considerably more involved than that of the steady model. Therefore, a brief summary of the modelling is provided here. The unsteady aerodynamics model is programmed in the following state-space form:

$$\begin{aligned} \dot{x} &= Ax + Bu \\ y &= Cx + Du \end{aligned} \tag{1}$$

The state matrix A is a square matrix that may be represented as follows:

$$A = \begin{bmatrix} A_{1,1} & \cdots & A_{1,15} \\ \vdots & \ddots & \vdots \\ A_{15,1} & \cdots & A_{15,15} \end{bmatrix} \tag{2}$$

where the non-zero terms are defined as follows:

$$\begin{gathered} A_{1,1} = \frac{-2V\beta^2 b_1}{c_{aero}};\ A_{2,2} = \frac{-2V\beta^2 b_2}{c_{aero}};\ A_{3,3} = \frac{-1}{T_\alpha};\ A_{4,4} = \frac{-1}{T_\alpha};\ A_{5,5} = \frac{-1}{T_{\alpha_M} b_3};\ A_{6,6} = \frac{-1}{T_{\alpha_M} b_4}; \\ A_{7,7} = \frac{-2V\beta^2 b_5}{c_{aero}};\ A_{8,8} = \frac{-1}{T_{q_M}};\ A_{9,10} = 1;\ A_{10,9} = -\left(\frac{2V}{c_{aero}}\right)^2 \beta^4 b_1 b_2;\ A_{10,10} = \frac{-2V(b_1+b_2)\beta^2}{c_{aero}}; \\ A_{11,11} = \frac{-1}{T_{x_i}};\ A_{12,12} = \frac{-1}{T_{\dot{x}_i}};\ A_{13,13} = \frac{-2V\beta^2 b_6}{c_{aero}};\ A_{14,14} = \frac{-1}{T_{x_i M}};\ A_{15,15} = \frac{-1}{T_{\dot{x}_i M}} \end{gathered} \tag{3}$$

here, V is airspeed, β is Prandtl-Glauert compressibility correction factor, c_{aero} is chord of an aerofoil, $b_1 \ldots b_6$ are exponents of indicial functions (Leishman 1988). Within the state matrix and later in the output matrix C, the following non-circulatory time constants (Leishman 1988) are also used:

$$\begin{gathered} T_\alpha = \frac{c_{aero} k_1}{a\left(1-M+\pi\beta M^2 (A_1 b_1 + A_2 b_2)\right)};\ T_{\alpha_M} = \frac{c_{aero}(A_3 b_4 + A_4 b_3)}{a b_3 b_4 (1-M)}; \\ T_q = \frac{2 c_{aero} k_2}{a\left(1-M+2\pi\beta M^2 (A_1 b_1 + A_2 b_2)\right)};\ T_{q_M} = \frac{7 c_{aero}}{a\left(15(1-M)+3\pi\beta M^2 b_5\right)}; \\ T_{x_i} = \frac{c_{aero}(1-x_e)}{a\left((1-M)+\frac{F_{10}}{\beta} M^2 (A_1 b_1 + A_2 b_2)\right)};\ T_{\dot{x}_i} = \frac{c_{aero}(1-x_e)^2}{2a\left((1-M)(1-x_e)+\frac{F_{11}}{\pi}\beta^2 M^2 (A_1 b_1 + A_2 b_2)\right)}; \\ T_{x_i M} = \frac{c_{aero}(1-x_e)(2+x_e)}{a\left(3(1-M)+2b_3 M^2 \beta (F_4 + F_{10})\right)};\ T_{\dot{x}_i M} = \frac{c_{aero}\left((1+x_e)^3 + 4 - 12x_e - \frac{3}{2}(1-x_e)^2\right)}{a\left(9(1-M)(1-x_e)+6b_3 M^2 \beta \left(F_1 - F_8 - F_4\left(\frac{1}{2}+x_e\right)+\frac{F_{11}}{2}\right)\right)} \end{gathered} \tag{4}$$

here $A_1 \ldots A_4$ are the coefficients of the various indicial functions (Leishman 1988), a is the speed of sound, M is the Mach number, $F_1 \ldots F_{11}$ are wing control surface geometric properties (Theodorsen 1949), x_e represents the hinge location of control surface as a percentage of chord. The input matrix B takes the following form:

$$B = \begin{bmatrix} B_{1,1} & \cdots & B_{1,4} \\ \vdots & \ddots & \vdots \\ B_{15,1} & \cdots & B_{15,4} \end{bmatrix} \tag{5}$$

The non-zero terms of the matrix B are as follows:

$$\begin{gathered} B_{1,1} = 1;\ B_{1,2} = \frac{c_{aero}}{2V};\ B_{2,1} = 1;\ B_{2,2} = \frac{c_{aero}}{2V};\ B_{3,1} = 1;\ B_{4,2} = 1;\ B_{5,1} = 1;\ B_{6,1} = 1;\ B_{7,2} = \frac{c_{aero}}{V}; \\ B_{8,2} = \frac{c_{aero}}{V};\ B_{9,3} = 0;\ B_{10,3} = \frac{F_{10}}{\pi};\ B_{10,4} = \frac{c_{aero}F_{11}}{4\pi V};\ B_{11,3} = 1;\ B_{12,4} = \frac{c_{aero}e^{1-x_e}}{2V};\ B_{13,3} = -\frac{F_4+F_{10}}{2\pi\beta}; \\ B_{13,4} = \frac{c_{aero}\left(2F_1-2F_8+F_{11}-F_4(1+2x_e)\right)}{8V\pi\beta};\ B_{14,3} = 1;\ B_{15,4} = 1 \end{gathered} \tag{6}$$

The output matrix C is represented in the following form:

$$C = \begin{bmatrix} C_{1,1} & \cdots & C_{1,15} \\ \vdots & \ddots & \vdots \\ C_{4,1} & \cdots & C_{4,15} \end{bmatrix} \tag{7}$$

The non-zero terms of the matrix C are as follows:

$$\begin{gathered} C_{1,1} = \frac{2V\beta^2A_1b_1}{c_{aero}};\ C_{1,2} = \frac{2V\beta^2A_2b_2}{c_{aero}};\ C_{1,9} = \left(\frac{2V}{c_{aero}}\right)^2\beta^4b_1b_2;\ C_{1,10} = \frac{2V\beta^2(A_1b_1+A_2b_2)}{c_{aero}};\ C_{2,1} = 0; \\ C_{2,2} = 0;\ C_{2,7} = \frac{-2V\beta^2b_5}{16c_{aero}};\ C_{2,13} = \frac{V\beta^2b_6}{c_{aero}};\ C_{3,3} = \frac{-4}{T_\alpha M};\ C_{3,4} = 0;\ C_{3,11} = \frac{-2(1-x_e)}{T_{x_i}M};\ C_{3,12} = 0; \\ C_{4,5} = \frac{A_3}{b_3T_{\alpha_M}M};\ C_{4,6} = \frac{A_4}{b_4T_{\alpha_M}M};\ C_{4,8} = 0;\ C_{4,14} = \frac{(1-x_e)(2+x_e)}{2T_{x_iM}M};\ C_{4,15} = 0 \end{gathered} \tag{8}$$

The feedthrough matrix D takes the following form:

$$D = \begin{bmatrix} D_{1,1} & \cdots & D_{1,4} \\ \vdots & \ddots & \vdots \\ D_{4,1} & \cdots & D_{4,4} \end{bmatrix} \tag{9}$$

And its non-zero terms are as follows:

$$D_{3,1} = \frac{4}{M};\ D_{3,3} = \frac{2(1-x_e)}{M};\ D_{4,1} = -\frac{1}{M};\ D_{4,3} = -\frac{(1-x_e)(2+x_e)}{2M} \tag{10}$$

The state vector x and input vector u are as follows:

$$\boldsymbol{x} = [x_1 \quad x_2 \quad x_3 \quad \ldots \quad x_n]^T \tag{11}$$

$$\boldsymbol{u} = [u_1 \quad u_2 \quad u_3 \quad u_4]^T \tag{12}$$

where n is a number of states.

Each aerodynamic node has a 15 element state vector $\boldsymbol{x}$ associated with it, together with an input vector $\boldsymbol{u}$ consisting of angle of attack, angle of control surface and their rates of change (Andrews 2011, Lone 2013). For the AX-1 model, the surfaces generating lift are modelled using 58 aerodynamic nodes that result in 870 unsteady aerodynamic states.

Steady aerodynamic coefficients for each section of the lifting surfaces are found from pre-programmed look-up tables (LUTs). Therefore, parameters such as viscous drag, zero lift drag, aerofoil profile drag and zero lift pitching moment coefficients and profile drag increase due to flaps are obtained through simple interpolation for a specified Mach number and Reynolds number. To take into account 3D effects, an indicial angle of attack (α_{ind}) is added to steady state angle of attack (α) and effective angle of attack (α_{eff}) is calculated:

$$\alpha_{eff} = \alpha + \alpha_{ind} \tag{13}$$

The modified strip theory is then applied to provide forces acting on aerodynamic surfaces in the wind axes system. These are transferred into the body axes system via the application of the following direction cosine matrix (DCM) that considers local deformation along with the relative changes in the orientation of the two axes systems:

$$DCM = \begin{bmatrix} cos\theta_i cos\lambda_i & cos\lambda_i sin\theta_i siny\gamma_i - sin\lambda_i cos\gamma_i & cos\lambda_i sin\theta_i cos\gamma_i + sin\lambda_i siny\gamma_i \\ cos\theta_i sin\lambda_i & siny\gamma_i sin\theta_i sin\lambda_i + cos\gamma_i cos\lambda_i & sin\lambda_i sin\theta_i cos\gamma_i - cos\lambda_i siny\gamma_i \\ -sin\theta_i & cos\theta_i siny\gamma_i & cos\gamma_i cos\theta_i \end{bmatrix} \tag{14}$$

here θ_i is local twist angle, λ_i is local sweep angle, γ_i is local dihedral angle. The various axes systems used in the model are shown in Fig. 4.

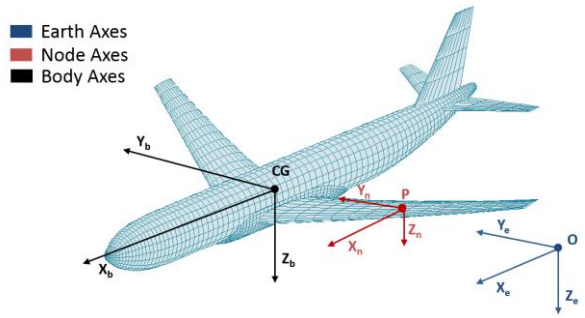

Fig. 4. Different axes systems used in the model.

The aerodynamic model also estimates the wing downwash effect on the tailplanes. Downwash circulation strength (Γ) is calculated as follows to estimate this influence:

$$\Gamma = sV\boldsymbol{A}(\alpha_{ind} - \alpha_{C_{L=0}}) \tag{15}$$

here s is span of a wing, $\boldsymbol{A}$ is coefficients matrix of modified strip theory, $\alpha_{C_{L=0}}$ is zero lift angle of attack. Circulation Γ is then evaluated through a reduced order state-space model to get the indicial angle of attack for the tailplane. This implementation of modified strip theory and unsteady aerodynamic modelling has been found to provide a satisfactory balance between precision and computational cost (Andrews 2011).

1.2. Fuselage and engines modelling

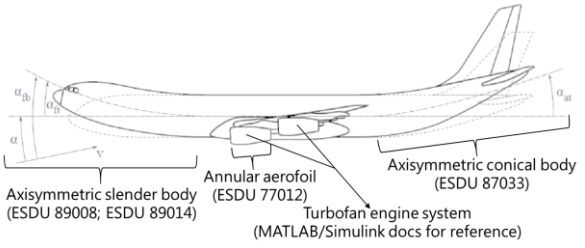

Fig. 5. Flexible fuselage and engines modelling.

The fuselage and engines make a significant contribution of forces and moments acting on aircraft. The sketch of the fuselage and engines with corresponding sources of modelling methods is shown in Fig. 5.

For aircraft such as the Airbus A340 or the Boeing 777 fuselage flexibility effects on flight dynamics and handling qualities cannot be ignored. Within this framework, fuselage flexibility is taken into account through the definition of elastic angles of attack and sideslip. The fuselage is divided into three parts – the nose, the tail and the central section which consists of the wing fuselage junction. Flexibility is considered via changes in angles of attack and sideslip for the nose and tail parts due to their deflection as shown in Fig. 5. The forebody of the fuselage is modelled as an axisymmetric slender body (see ESDU 89008 and ESDU 89014) and the aftbody is modelled as an axisymmetric conical body (see ESDU 87033).

Engine dynamics are also modelled in this framework. The forces and moments from each engine is split into two parts – nacelle aerodynamics and the thrust producing unit. Nacelles are modelled as annular aerofoils (see ESDU 77012). Flexibility is taken into account, as in the case of fuselage, through additional terms for angles of attack and sideslip. Within the AX-1 implementation, the thrust producing unit is modelled as a turbofan engine. Forces and moments of each engine are calculated in the engine axes system. However, these are transferred to the body axes system to be included in total forces and moments.

1.3. Differences between aerodynamic and structural frames

Forces and moments from aerodynamic surfaces, fuselage and engines are calculated at aerodynamic nodes and structural forces and moments are evaluated at the structural nodes. Therefore, an aeroelastic simulation requires a transformation of aerodynamic forces and moments in aerodynamic nodes to structural nodes and vice versa. However, a typical implementation such as the AX-1 model, has aerodynamic contributions being calculated at a higher resolution than the structural dynamic contributions. Thus, the number of aerodynamic nodes often exceeds the number of structural nodes and these nodes are not collocated in space. Loads therefore need to be transformed from the aerodynamic frame to the structural frame and it is very important to analyse the difference between those two frames.

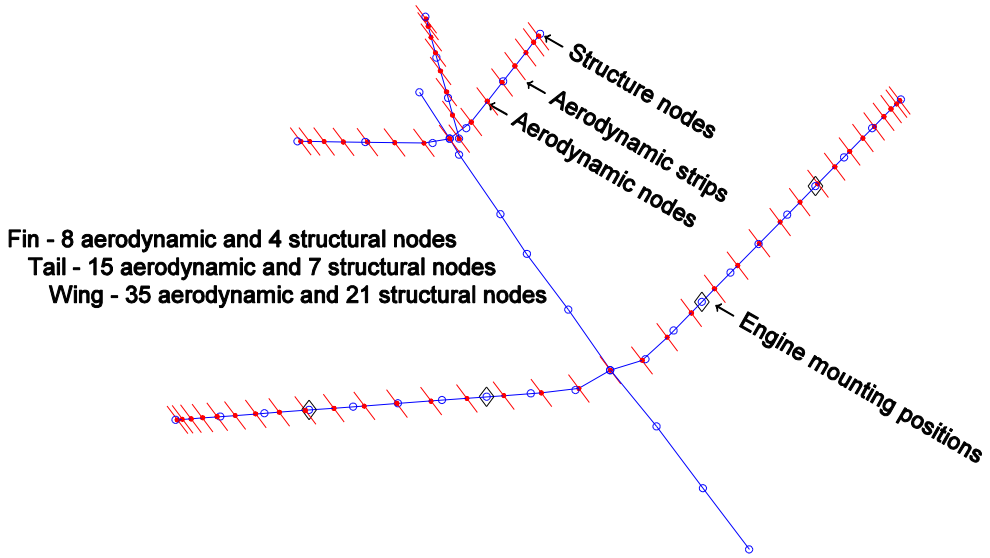

Fig. 6. Scheme of AX-1 model aerodynamic and structural frames.

Fig. 6 shows the scheme as applied to the AX-1 model. Along the wing of AX-1 there are 35 aerodynamic nodes, which correspond to 35 aerodynamic strips. It is shown (Fig. 7) that this is the optimal number of strips providing the desired balance between model accuracy and computational cost. The same analysis was done for the tailplane and fin, resulting in the selection of 15 and 8 aerodynamic strips respectively. On the other hand, structural layout is modelled with 21, 7 and 4 nodes for the wing, fuselage and tailplane respectively. 10 nodes are used for fuselage modelling, 2 of which coincide with central nodes of wing and tailplane. Hence, additional operations are done converting aerodynamic loads to structural loads and then structural frame deflections to aerodynamic frame deflections.

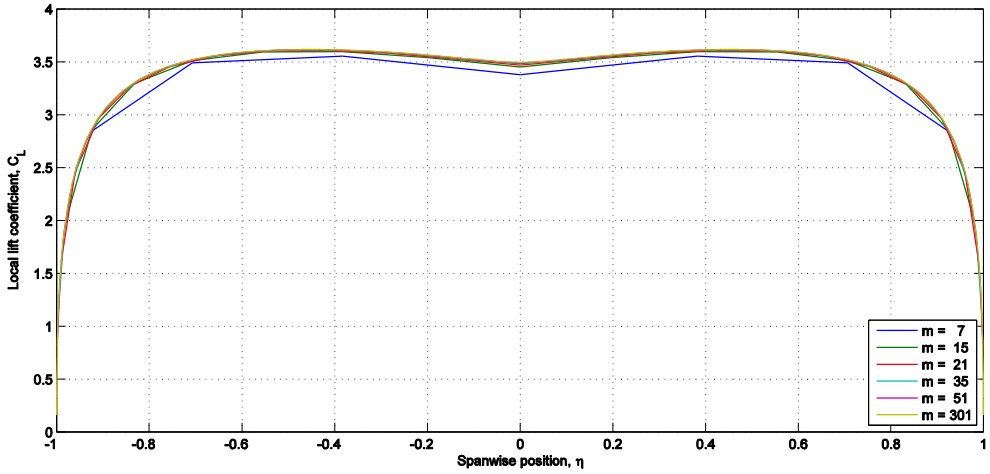

Fig. 7. Local lift coefficient C_L resolution with different number of aerodynamic strips (Andrews and Cooke 2011).

1.4. Structural modelling

Structural modelling is done in a structural dynamics block and the process is shown in Fig. 8. This block converts aerodynamic and gravitational loads to structural loads. The structural dynamics for the AX-1 implementation is done in the modal domain, thus stiffness and mass matrices are generated to obtain structural mode shapes. The first structural 4 modes of the AX-1 model are shown in Fig. 9.

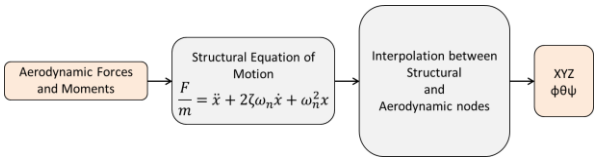

Fig. 8. Structural dynamics block of CA^{2}LM framework.

The following structural equations of motion are solved to acquire modal accelerations ($\ddot{x}$), velocities ($\dot{x}$) and displacements (x):

$$\frac{F_i}{m_i} = \ddot{x}_i + 2\zeta\omega_n\dot{x}_i + \omega_n^2 x_i \tag{16}$$

here F_i is modal force, m_i is modal mass, ω_n is modal natural frequency, ζ is damping ratio, i is a number of mode.

Finally, transition from modal to nodal displacements, velocities and accelerations is done. Results of each mode influence are acquired and summed with other modal influences to give the resultant displacements, velocities and accelerations. The AX-1 implementation only considers the first 12 modes because the model aims to analyse flight dynamics phenomena that are typically at low frequencies.

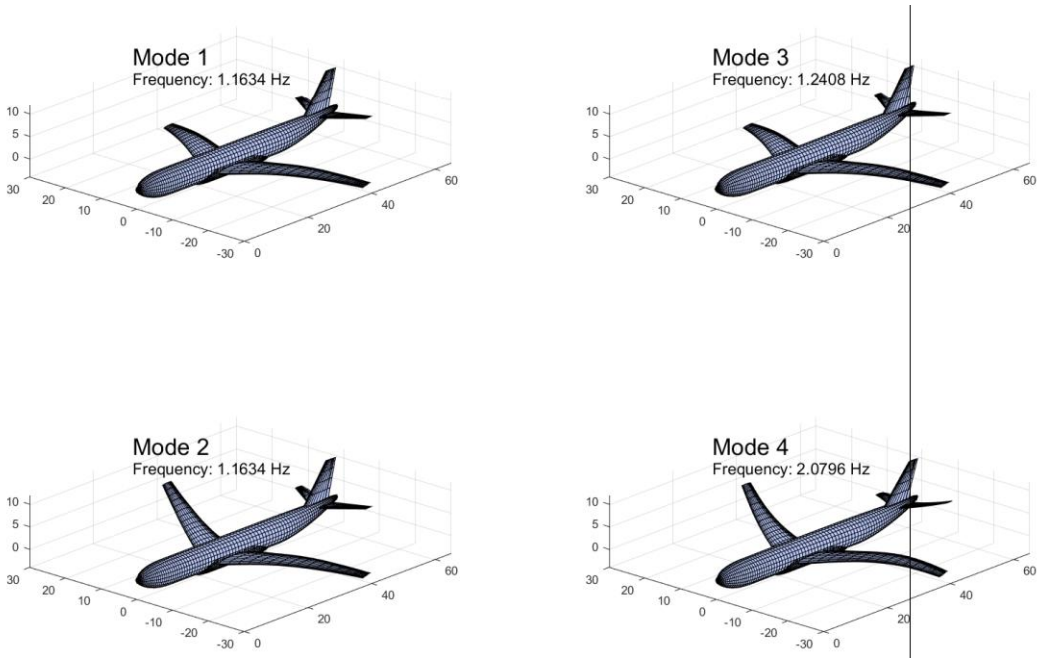

Fig. 9. First 4 mode shapes of the AX-1 model structure.

It is important to notice that only small deflections (less than 10% of a wing span) are modelled within CA^{2}LM framework as it is assumed that properties of each beam vary linearly. However, recent developments in highly flexible aircraft (Patil and Hodges 2006) have introduced wing deflections of more than 25% of wing semi-span. As a result a non-linear approach to model structural dynamics is currently under investigation.

1.5. Equations of motion

Forces and moments acting on the aircraft are concentrated at the centre of gravity (CG), about which accelerations, attitude, position and velocities are calculated. However, airframe flexibility is taken into account through the recalculation of moments for a constantly changing CG position. This method has been considered as an appropriate way of taking flexibility effects into account (as explained in Section 1.4). The equations solved for body forces ($\boldsymbol{F}_b$) and moments ($\boldsymbol{M}_b$) are in vector form as follows:

$$\boldsymbol{F}_b = m\left(\dot{\boldsymbol{V}}_b + \boldsymbol{\omega} \times \boldsymbol{V}_b\right) \tag{17}$$

$$\boldsymbol{M}_b = I\dot{\boldsymbol{\omega}} + \boldsymbol{\omega} \times (I\boldsymbol{\omega}) \tag{18}$$

here $\boldsymbol{F}_b = [F_x\ F_y\ F_z]^T$, m is mass of an aircraft, $\boldsymbol{V}_b = [V_x\ V_y\ V_z]^T$ is linear velocities in x-, y- and z- axes, $\boldsymbol{\omega} = [p\ q\ r]^T$ is angular velocities around x-, y- and z- axes, $\boldsymbol{M}_b = [M_x\ M_y\ M_z]^T$, I is inertia matrix. For further reference on equations of motion the reader is referred to Stengel (Stengel 2004) and Cook (Cook 2007). Yet, it should be noted that significant changes in CG position are expected because of high structural deformations. A constantly changing CG position will result in a time-varying inertia tensor I. Hence, a contribution of each node should be taken into account in the equations of motion and a new approach is currently under development.

1.6. Gravity and atmosphere modelling

Gravity is modelled according to WGS-84 reference (*WGS-84* 1991). Gravitational constant (γ_h) is calculated using the following equation:

$$\gamma_h = \gamma_e \frac{1+k\sin^2\phi}{\sqrt{1-e^2\sin^2\phi}}\left[1 - \frac{2}{a}\left(1 + f + \frac{\omega^2 a^2 b}{GM} - 2f\sin^2\phi\right)h + \frac{3}{a^2}h^2\right] \tag{19}$$

here γ_e is theoretical gravity at the equator, k is theoretical gravity formula constant, e is first ellipsoidal eccentricity, φ is geodetic latitude, a is semi-major axis, f is ellipsoidal flattening, ω is angular velocity of the Earth, b is semi-minor axis, GM is Earth's gravitational constant, h is height. The gravitational constant is then applied at the CG position for solving equations of motion. Additionally it is applied to each structural node to solve structural equation of motion (see

Section 1.4). Atmospheric properties such as air density and temperature are modelled as International Standard Atmosphere (ISA) according to ESDU 77021.

2. Case studies utilising CA^{2}LM framework

This sections briefly presents two case studies demonstrating the capabilities of the CA^{2}LM framework. The first case study focuses on handling qualities analysis and the second demonstrates the capability of performing failure case assessments. Both case studies are based on the AX-1 model which is representative of a large transport aircraft.

2.1. Time domain handling qualities analysis

The Gibson Dropback Criterion (Gibson 1982) is a well-known approach developed to predict longitudinal handling qualities and assist in the design of command and stability augmentation systems. The key advantage of this approach is that it is based in the time domain and so effects of nonlinear dynamics arising due to nonlinear flight control can be considered in handling qualities analysis. Such effects cannot be captured through approaches based on low order equivalent systems (LOES). The key parameters for evaluating the Dropback criterion are:

1. *Pitch rate overshoot ratio, which is expressed as a ratio between maximum pitch rate (q_m) and steady state pitch rate (q_{ss}).*
2. *Attitude dropback (DB) to steady state pitch rate (q_{ss}) ratio.*

These parameters are illustrated graphically in Fig. 10. The criterion is based on these ratios and extensive pilot opinion gathered to outline regions of satisfactory and undesirable response characteristics as shown in Fig. 11. The boundaries shown in Fig. 11 are based on research conducted by Mooij (Mooij 1985) which focused on large transport aircraft.

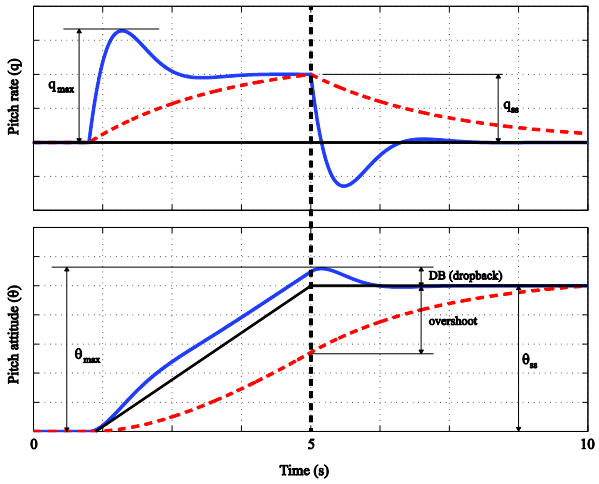

Fig. 10. Visualisation of q_m, q_{ss} and *DB* terms used in the Gibson Dropback criterion.

In this case study, the AX-1 model was trimmed at an altitude of *10000 ft* and the Dropback criterion was evaluated at several airspeeds. This was carried by specifying an elevator doublet input of ±*5*°. Fig. 11 shows the variation of longitudinal handling qualities with varying airspeed. It should be noted that no stability augmentation system has been implemented, and consequently the majority of the cases are not in the satisfactory region. However, at airspeeds of *180 m/s*, *190 m/s* and *200 m/s* the response of the aircraft is within the satisfactory region.

2.2. Aileron soft failure simulation

A control surface failure scenario is one of many extreme cases that need to be considered for flight loads evaluation. Here a soft aileron failure is simulated where the port aileron undergoes an actuation failure whilst starboard aileron remains in the original trim setting. The main results obtained from the simulation of the AX-1 model are shown in Fig. 12. The port aileron is forced to effectively undergo a limit cycle oscillation at a constant frequency of *1.16 Hz*, which corresponds to the first wing structural bending mode. The amplitude of this oscillation is set to ±15°.

The frequency content of the roll rate (*p)* and yaw rate (*r)* signals show that the failure has excite a low frequency lateral-directional mode corresponding to periods of T_p*=10.24 sec* and T_r*=10.92 sec* in roll and yaw respectively. These correspond to the usual frequencies of the aircraft's Dutch roll mode. The highest peaks, just above *1 Hz*, are the direct

result of the simulated aileron forcing function. The load factor (n) only exhibits large transients when the aileron failure is initiated.

Fig. 13 shows the frequency content of the wing root bending moment M_{root} at different aileron excitation frequencies. At a frequency of *1.245 Hz*, slightly higher than the frequency of the first structural mode of the wing (*1.1634 Hz*), the first aeroelastic mode appears and a resulting resonance is observed. Upon magnification (bottom right subfigure) another two peaks can be observed at *2.5 Hz* and *3 Hz*. These correspond to aeroelastic modes associated with the 5th and 11th structural wing bending modes. At the frequency of *0.9 Hz* M_{root} is higher than at the frequency of *1.1 Hz*, which can be explained by the fact that the forcing function frequency is getting closer to rigid body frequencies.

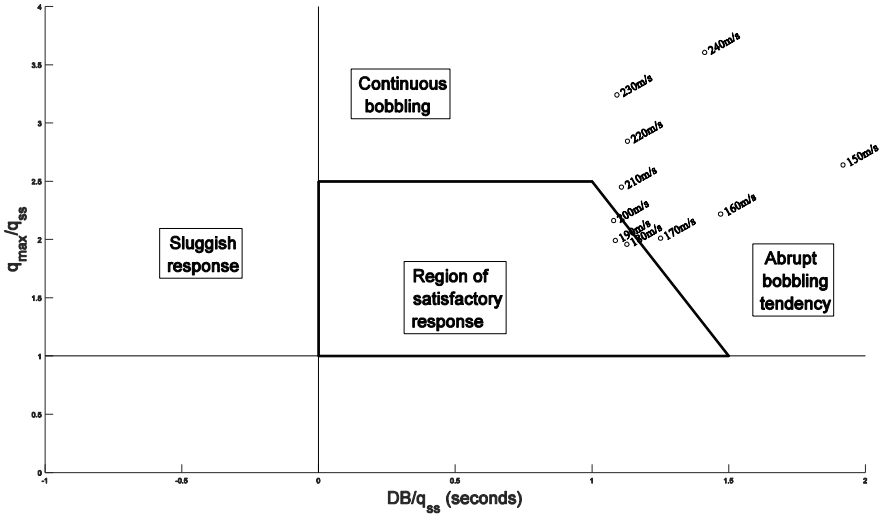

Fig. 11. Effect of airspeed on longitudinal handling qualities of AX-1 model.

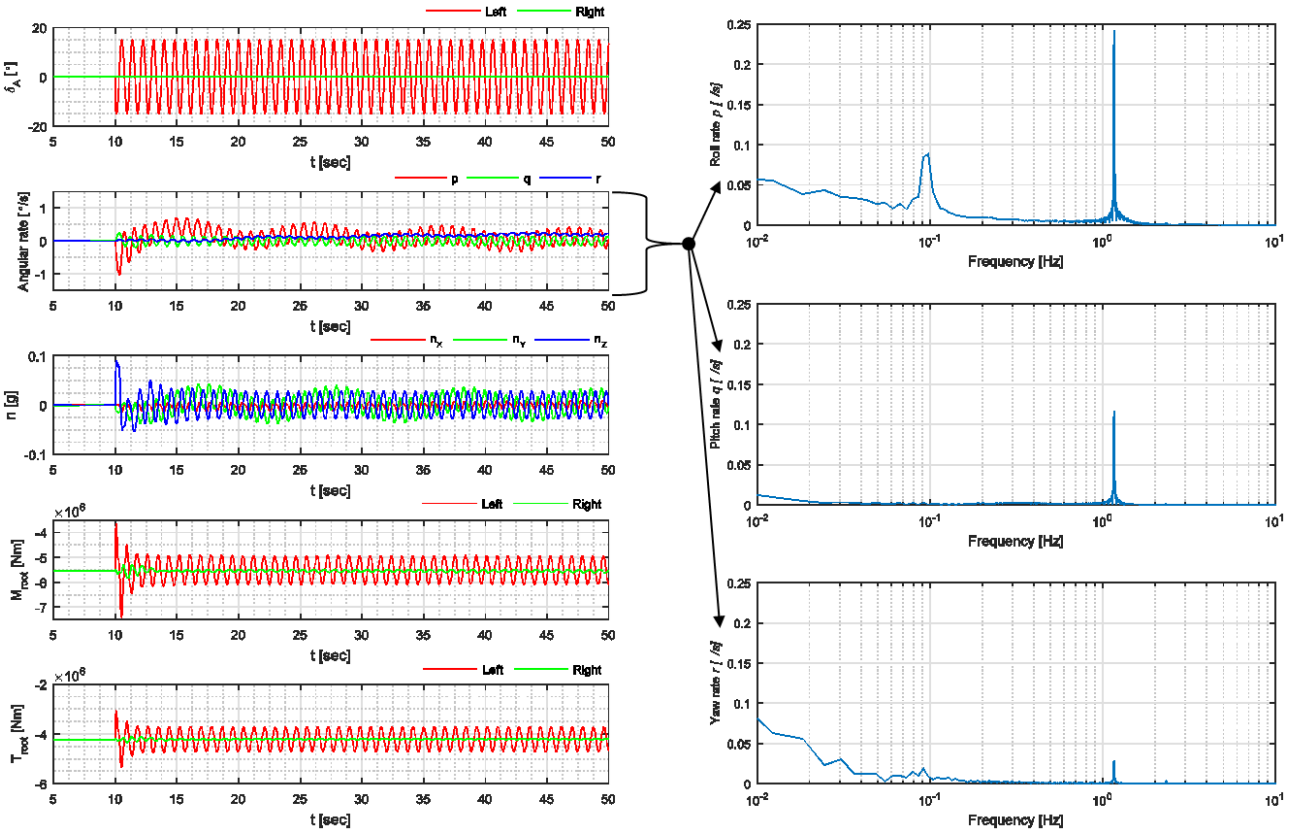

Fig. 12. Ailerons deflection δ_A, angular rate, load factor n, wing root bending moment M_{root} and wing root torsion T_{root} and roll, pitch and yaw rates at aileron excitation frequency *f=1.1634 Hz.*

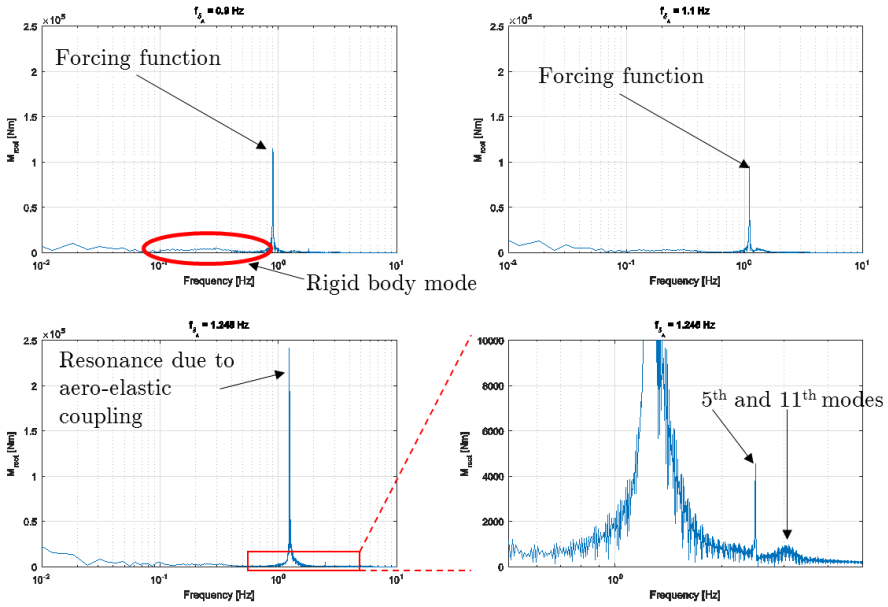

Fig. 13. Wing root bending moment M_{root} at different aileron excitation frequencies.

Conclusions

A brief overview of the CA^{2}LM framework designed to model flexible aircraft has been presented in this paper. Structural deformations are obtained through a linear modal formulation of the aircraft structure. Assumption of linearity limits the model to small deformations that are less than 10% of the wing semi-span. The aerodynamics are modelled by coupling steady modified strip theory with the Leishman-Beddoes unsteady model in state space form. The CA^{2}LM framework effectively combines these methods in a MATLAB/Simulink environment. The capabilities of such an environment is demonstrated through two case studies. These cases have focused on the AX-1 model which represents a generic large transport aircraft. The first case study focuses on the handling qualities analysis based on the Dropback criterion. It demonstrates that the AX-1 model response to longitudinal control input is unsatisfactory without stability augmentation system. The second case study simulates a port aileron failure case and its impact on structural loads. It shows that coupling between aeroelastic modes and rigid body flight dynamic modes appear when the aileron undergoes a limit cycle oscillation at a slightly higher frequency than the first wing bending mode.

Recent developments in highly flexible aircraft have introduced wing deflections of more than 25% of wing span. Thus, a new approach to structural modelling is currently being developed. Moreover, such a flexible aircraft cannot be assumed as a rigid body when solving the flight dynamic equations of motion. Hence, a new approach of including additional terms due to flexibility into equations of motion is being investigated.

Acknowledgements

Author would like to acknowledge Stuart P. Andrews for developing the AX-1 aircraft model and tools for its analysis during his PhD degree at Cranfield University. These tools were a basis for developing a current CA^{2}LM framework.

References

Andrews, S.P., 2011. Modelling and simulation of flexible aircraft : handling qualities with active load control (Bibliographies). Cranfield University.

Cook, M.V., 2007. Flight dynamics principles: a linear systems approach to aircraft stability and control, 2nd ed. ed, Elsevier aerospace engineering series. Butterworth-Heinemann/Elsevier, Oxford [UK] ; Burlington, MA.

Cooper, J.E., Gaitonde, A., Jones, D., Lowenberg, M.H., Sartor, P., Lemmens, Y., 2016. Aircraft Loads Prediction using Enhanced Simulation (ALPES). American Institute of Aeronautics and Astronautics. doi:10.2514/6.2016-1571

DeYoung, J., Harper, C.W., 1948. Theoretical symmetric span loading at subsonic speeds for wings having arbitrary plan form (No. NACA-TR-921).

DoD World Geodetic System 1984: Its definition and Relationship with Local Geodetic Systems (No. TR8350.2), 1991. . National Imagery and Mapping Agency.

European Commission, 2011. Flightpath 2050: Europe's vision for aviation. Publications Office of the European Union, Luxembourg.
Gibson, J.C., 1982. Criteria For Handling Qualities Of Military Aircraft (No. AGARD-CP-333). AGARD, Neuilly-sur-Seine.
Kier, T., Looye, G., Hofstee, J., 2005. Development of Aircraft Flight Loads Analysis Models with Uncertainties for Pre-Design Studies, in: IFASD 2005. München.
Leishman, J.G., 1988. Validation of approximate indicial aerodynamic functions for two-dimensional subsonic flow. Journal of Aircraft 25, 914–922. doi:10.2514/3.45680
Lindhorst, K., Haupt, M.C., Horst, P., 2014. Efficient Surrogate Modelling of Nonlinear Aerodynamics in Aerostructural Coupling Schemes. AIAA Journal 52, 1952–1966. doi:10.2514/1.J052725
Lone, M., 2013. Pilot modelling for airframe loads analysis (Bibliographies). Cranfield University.
Mooij, H.A., 1985. Criteria for Low-Speed Longitudinal Handling Qualities. Springer Netherlands, Dordrecht.
Morelli, E., 2002. System Identification Programs for AirCraft (SIDPAC). American Institute of Aeronautics and Astronautics. doi:10.2514/6.2002-4704
Palacios, R., Cesnik, C., 2008. Low-Speed Aeroelastic Modeling of Very Flexible Slender Wings with Deformable Airfoils. American Institute of Aeronautics and Astronautics. doi:10.2514/6.2008-1995
Palacios, R., Murua, J., Cook, R., 2010. Structural and Aerodynamic Models in Nonlinear Flight Dynamics of Very Flexible Aircraft. AIAA Journal 48, 2648–2659. doi:10.2514/1.J050513
Patil, M.J., Hodges, D.H., 2006. Flight Dynamics of Highly Flexible Flying Wings. Journal of Aircraft 43, 1790–1799. doi:10.2514/1.17640
Simpson, R.J., Palacios, R., Goulart, P.J., 2015. Integrated Flight Dynamics and Aeroelasticity of Flexible Aircraft with Application to Swept Flying Wings. American Institute of Aeronautics and Astronautics. doi:10.2514/6.2015-0183
Stengel, R.F., 2004. Flight dynamics. Princeton University Press, Princeton, NJ.
Theodorsen, T., 1949. General Theory of Aerodynamic Instability and the Mechanism of Flutter (No. NACA-TR-496).
Tollefson, J., 2016. UN agency proposes greenhouse-gas standard for aircraft. Nature 530, 266–266. doi:10.1038/nature.2016.19336
Wang, F., Huo, S., Qiao, S., Zhang, J., Yue, Z., 2015. An effective computer modelling approach to the study of aeroelastic characteristics of an aircraft composite wing with high aspect ratio. Mathematical and Computer Modelling of Dynamical Systems 21, 58–76. doi:10.1080/13873954.2014.903283
Weissinger, J., 1947. The Lift Distribution of Swept-Back Wings (No. NACA-TM-1120).